Chemical Science

ROYAL SOCIETY OF CHEMISTRY

EDGE ARTICLE

View Article Online
View Journal | View Issue



Cite this: *Chem. Sci.*, 2025, **16**, 22456

All publication charges for this article have been paid for by the Royal Society of Chemistry



# Palladium-catalysed asymmetric annulations of Morita–Baylis–Hillman carbonates with allenes or alkenes *via* migratory insertion

Jin-Yu Huang,†[a] Xin-Ting Qin,†[a] Han-Wen Rao,[a] Zhi-Chao Chen,*[a] Lei Zhu,[b] Qin Ouyang,*[b] Wei Du[a] and Ying-Chun Chen*[a]

Received 8th September 2025
Accepted 14th October 2025

DOI: 10.1039/d5sc06910f

rsc.li/chemical-science

As one of the most versatile intermediates in organic synthesis, π-allylpalladium complexes have been extensively exploited in allylic alkylation reactions with a wide range of nucleophiles. In contrast, their engagement in the migratory insertion process remains significantly underdeveloped. Here we demonstrate that the π-allylpalladium intermediates derived from $Pd^0$ and Morita–Baylis–Hillman (MBH) carbonates of activated ketones can isomerize to the corresponding $\eta^1$-form when stabilised by a pendent carbonyl group, and undertake migratory insertion into various allenes and even styrene-type alkenes efficiently. Subsequent vinylogous deprotonation of the newly formed multifunctional π-allylpalladium species followed by isomerization and intramolecular allylic alkylation leads to skeletally diverse (3 + 2) adducts with high levels of regio- and stereoselectivity. This catalytic strategy not only achieves migratory insertion of non-zwitterionic π-allylpalladium intermediates, but also overcomes the inherent limitations that the MBH carbonates can only undergo annulations with electrophilic dipolarophiles *via* Lewis base catalysis. Mechanistic insights are further elucidated through comprehensive density functional theory calculation studies.

## Introduction

Owing to their ready availability and versatile reactivity, π-allylpalladium complexes have emerged as a type of cornerstone synthons in modern organic chemistry.[1] Such robust intermediates can be readily generated through various pathways, including the oxidative addition of $Pd^0$ to allylic derivatives,[2] as well as Pd-mediated C–H activation of alkenes[3] or hydropalladation [or $Pd^0$-promoted protonation] of polyunsaturated hydrocarbons.[4] Traditionally, π-allylpalladium species are utilised as electrophiles in the Tsuji–Trost allylic alkylation reaction (Scheme 1a, path A).[5] Alternatively, π-allylpalladium species occasionally serve as nucleophiles to couple with electrophiles in the presence of suitable reductants (Scheme 1a, path B).[6]

Unlike aryl-$Pd^{II}$ or alkenyl-$Pd^{II}$ intermediates,[7] allyl-$Pd^{II}$ species were rarely applied in migratory insertion reactions. In fact, in the 1970s, Powell conceptually demonstrated that π-allylpalladium complexes could undertake migratory insertion into 1,3-dienes through transient formation of corresponding $\eta^1$-intermediates (Scheme 1a, path C).[8] However, synthetic transformations of π-allylpalladium complexes into value-added products *via* migratory insertion have been scarcely explored ever since, probably due to the reluctant isomerization of thermodynamically more stable $\eta^3$-allylpalladium complexes to their $\eta^1$-ones. A major breakthrough was achieved by Trost in 2018, who uncovered that specific oxatrimethylene–methane–palladium species **INTA** underwent a cascade migratory insertion/allylation reaction with 1,3-dienes to furnish *cis*-fused methylene tetrahydrofurans (Scheme 1b).[9] Experimental and density functional theory (DFT) studies verified that the preinstalled ester group was instrumental for the desired migratory insertion, which not only stabilized **INTA** in a $\eta^1$-form, but also effectively lowered the LUMO (lowest unoccupied molecular orbital) energy, rendering them more closely with the HOMO (highest occupied molecular orbital) energy of 1,3-diene partners.[10] Later, Garg and Ma have accomplished migratory insertion of π-allylpalladium-contained 1,4-*C*,*N*-dipoles **INTB** into strained cyclic allenes and terminal allenes, respectively.[11] Recently, we realised migratory insertion of azapalladacycles **INTC**, *in situ* generated from electron-deficient 1-azadienes and $Pd^0$ *via* oxidative addition, into racemic internal allenes, and enantioselective and regiodivergent allylation could be obtained to deliver tetrahydropyridine products.[12] Despite such impressive progress, only limited and specially tailored zwitterionic π-allylpalladium complexes were successfully utilised in

[a]*Key Laboratory of Drug-Targeting and Drug Delivery System of the Education Ministry and Sichuan Province and Sichuan Research Center for Drug Precision Industrial Technology, West China School of Pharmacy, Sichuan University, Chengdu 610041, China. E-mail: chenzhichao@scu.edu.cn; ycchen@scu.edu.cn*

[b]*College of Pharmacy, Third Military Medical University, Shapingba, Chongqing 400038, China. E-mail: ouyangq@tmmu.edu.cn*

† J.-Y. Huang and X.-T. Qin equally contributed to this work.

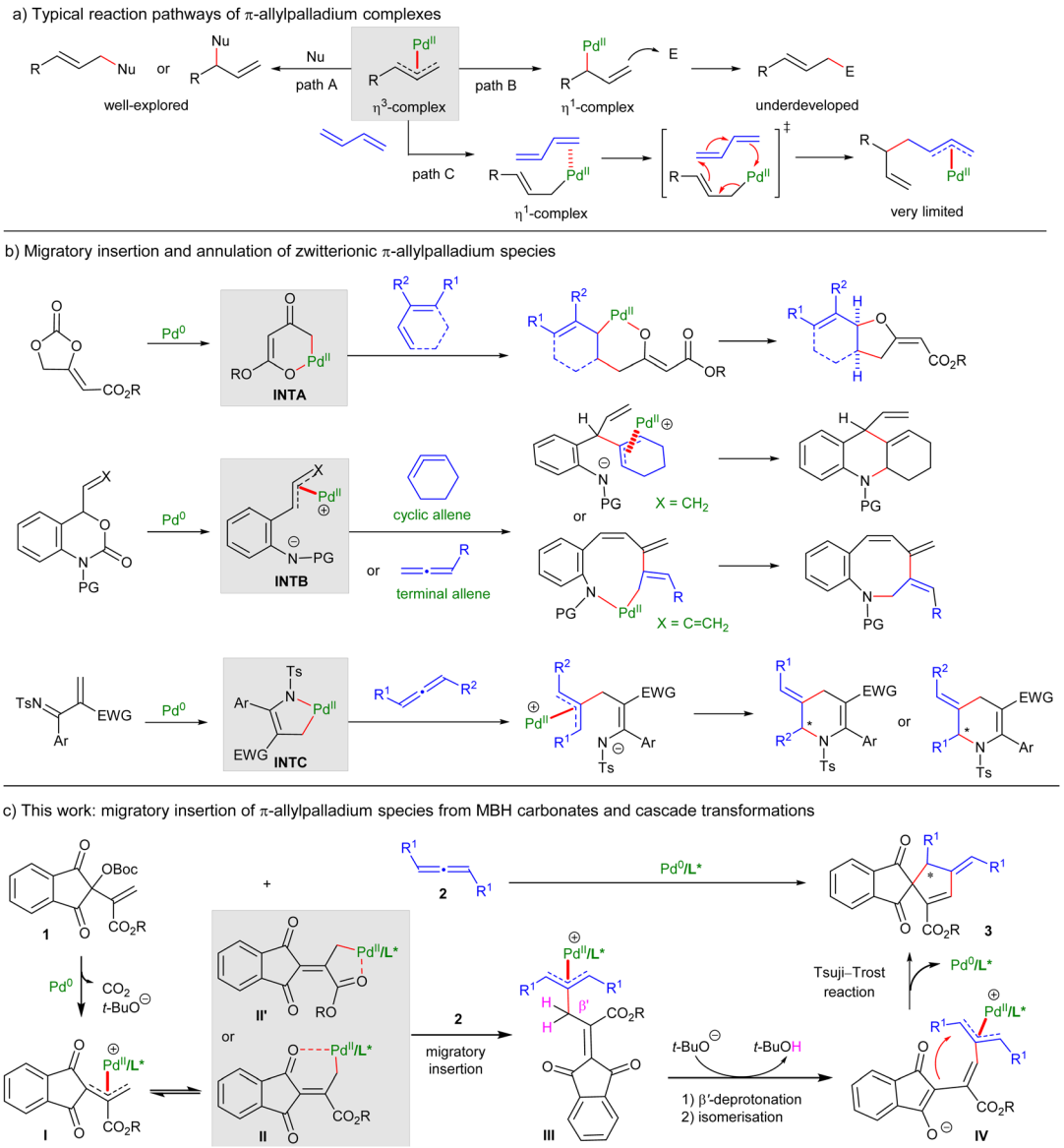


Scheme 1 Development of migratory insertion reactions of π-allylpalladium-based species.

migratory insertion reactions. Alternative application of novel functionalised π-allylpalladium species, especially the non-zwitterionic ones, to undergo migratory insertion reactions with diverse unsaturated systems would be highly desirable.

The Morita–Baylis–Hillman (MBH) adducts, condensed from carbonyls and activated alkenes, have been widely used in annulations after conversion to zwitterionic allylic ylide species with organic Lewis bases, but their counterparts were inherently limited to electrophilic alkenes and dipoles.[13] We envisioned that functionalised MBH carbonates, such as ninhydrin-derived ones **1**, could be activated by $Pd^0$ to form $\eta^3$-allylpalladium complexes **I**.[14] The pendent carbonyl might serve as an additional coordinating site to facilitate the isomerisation of **I** to the $\eta^1$-form **II** or **II′**, which would help lower the LUMO energy and facilitate the migratory insertion into allenes **2** possibly. Notably, the vinylogous β′-protons of the resultant π-allylpalladium complexes **III** are highly acidic and could be readily deprotonated by the previously generated *t*-butoxide anion.[15] Subsequent isomerisation and intramolecular Tsuji–Trost reaction would finally furnish (3 + 2) cycloadducts **3**, even enantioselectively. This rational design would not only broaden the π-allylpalladium species suitable for migratory insertion reactions, but also introduce a novel catalytic strategy for the transformations of multifunctional MBH carbonates, allowing for their assemblies with electron-neutral unsaturated systems, which are not feasible *via* conventional Lewis base catalysis.

## Results and discussion

### Reaction optimisation

We initiated the investigation by examining the reaction between MBH carbonate **1a** and racemic internal allene **2a** in

Table 1 Condition optimisations of the asymmetric (3 + 2) annulations of MBH carbonates **1** and racemic allene **2a**[a]

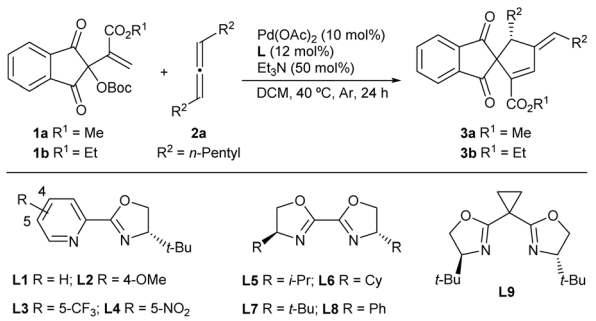


| Entry | [Pd] | L | Solvent | Yield[b] (%) | ee[c] (%) |
|---|---|---|---|---|---|
| 1[d] | $Pd(PPh_3)_4$ | — | DCM | **3a**, 18 | — |
| 2 | $Pd(OAc)_2$ | **L1** | DCM | **3a**, 30 | 66 |
| 3 | $Pd(OAc)_2$ | **L2** | DCM | **3a**, 70 | 61 |
| 4 | $Pd(OAc)_2$ | **L3** | DCM | **3a**, 80 | 70 |
| 5 | $Pd(OAc)_2$ | **L4** | DCM | **3a**, 84 | 73 |
| 6 | $Pd(OAc)_2$ | **L5** | DCM | **3a**, 89 | 81 |
| 7 | $Pd(OAc)_2$ | **L6** | DCM | **3a**, 86 | 82 |
| 8 | $Pd(OAc)_2$ | **L7** | DCM | **3a**, 76 | 87 |
| 9 | $Pd(OAc)_2$ | **L8** | DCM | **3a**, 81 | 33 |
| 10 | $Pd(OAc)_2$ | **L9** | DCM | **3a**, 35 | 5 |
| 11 | $Pd(OAc)_2$ | **L7** | DCE | **3a**, 63 | 85 |
| 12 | $Pd(OAc)_2$ | **L7** | MeOH | **3a**, 34 | 89 |
| 13 | $Pd(OAc)_2$ | **L7** | Toluene | **3a**, 17 | 89 |
| 14 | $Pd(OAc)_2$ | **L7** | THF | **3a**, 74 | 88 |
| 15[e] | $Pd(OAc)_2$ | **L7** | DCM | **3b**, 81 | 90 |
| 16[e] | $Pd(TFA)_2$ | **L7** | DCM | **3b**, 93 | 92 |
| 17[e] | $Pd_2(dba)_3$ | **L7** | DCM | **3b**, 70 | 81 |
| 18[e] | Pd(allyl)cp | **L7** | DCM | **3b**, 15 | 61 |
| 19[e,f] | $Pd(TFA)_2$ | **L7** | DCM | **3b**, 68 | 93 |
| 20[d,e] | $Pd(TFA)_2$ | **L7** | DCM | NR | — |
| 21[e,g] | $Pd(TFA)_2$ | **L7** | DCM | **3b**, 84 | 91 |

[a] Unless noted otherwise, the reaction was performed with MBH carbonate **1a** (0.1 mmol), racemic allene **2a** (0.2 mmol), [Pd] (10 mol%), **L** (12 mol%) and $Et_3N$ (0.05 mmol) in DCM (1.0 mL) at 40 °C for 24 h under Ar. [b] Yield of the isolated product. [c] Determined by HPLC analysis on a chiral stationary phase. [d] Without $Et_3N$. [e] **1b** (0.1 mmol) was used. [f] At rt. [g] With **2a** (0.1 mmol).

DCM at 40 °C under the catalysis of $Pd(PPh_3)_4$. To our delight, apparent conversions were observed to give the desired (3 + 2) annulation product **3a**, albeit in a low yield, as side reactions promoted by Lewis basic $PPh_3$ were also noted (Table 1, entry 1). Consequently, a series of chiral ligands in combination with $Pd(OAc)_2$ were examined for asymmetric induction. After screenings,[16] it was found that using pyridinyl-oxazoline **L1** exhibited fair catalytic efficiency and moderate enantioselectivity (entry 2). Introducing either electron-donating or withdrawing substituents into the pyridine skeleton (**L2**–**L4**) improved the yield significantly, but the enantioselectivity was unsatisfactory (entries 3–5). Chiral bisoxazolines **L5**–**L8** were applicable (entries 6–9), and a high ee value was obtained with **L7** having bulky *tert*-butyl groups (entry 8). Unfortunately, poor catalytic efficacy was observed with ligand **L9** (entry 10). Other solvents were tested but delivered diminished yields (entries 11–14). While slightly higher enantioselectivity was achieved by employing MBH carbonate **1b** from ethyl acrylate (entry 15), a quick survey of palladium sources revealed that $Pd(TFA)_2$ was a better choice (entries 16–18). Lowering the temperature resulted in a significantly reduced yield because of incomplete conversions (entry 19). A control experiment verified the necessity of $Et_3N$ (entry 20), which might act as a reductant to ensure the generation of reactive $Pd^0$ from the $Pd^{II}$ pre-catalyst.[17] It should be noted that a high yield was retained by employing 1.0 equivalent of allene **2a** (entry 21).

## Substrate scope investigation

Consequently, we first investigated the scope of MBH carbonates **1** in the reactions with racemic allene **2a** under the catalysis of $Pd(TFA)_2$/**L7**. As summarised in Scheme 2a, comparable good yields and enantioselectivity were obtained for products **3a–c** with diverse ester groups, whereas slightly diminished enantiocontrol was observed for products **3d** and **3e** from vinyl ketone-derived carbonates **1**. In addition, high yields and ee values were attained for the MBH carbonates **1** bearing either electron-rich or -deficient groups on the phenyl ring (products **3f–h**), even for the benzo[*f*]ninhydrin-derived one (product **3i**). Next, a variety of racemic symmetric allenes **2** were explored. As illustrated in Scheme 2b, a wide range of 1,3-dialkyl substituted allenes **2**, even those with various functionalities, all underwent the (3 + 2) annulations with MBH carbonate **1b** smoothly, producing **3j–r** in moderate to good yields with uniformly high enantioselectivity. Some allenes with drug motifs were also compatible (product **3s** and **3t**). In addition, cyclic allene worked well to yield product **3u** with moderate enantioselectivity. Notably, 1,3-diaryl-substituted allenes **2** were also applicable under the catalysis of $Pd(TFA)_2$/**L9**, giving corresponding product **3v–z** in moderate to high yields and enantioselectivity.

Encouraged by these results, we next turned our attention to explore the (3 + 2) annulations of the MBH carbonate **1b** with more challenging unsymmetrical allenes, as simultaneous control over enantio- and regioselectivity in the allylation step would be encountered. Delightfully, 1-aryl-, 1-alkoxyl- and 1-amino-substituted terminal allenes exhibited high reactivity in the assemblies with MBH carbonate **1b** under the catalysis of $Pd(TFA)_2$/**L10**, and products **4a–g** were generally furnished in outstanding yields and regioselectivity, whereas moderate to good ee values were obtained. Even a 1,1-disubstituted allene was compatible, affording product **4h** featuring a quaternary stereocenter with good data (Scheme 2c). Moderate regioselectivity could be achieved with 1-aryl-3-alkyl-allene, but both products **5a** and **5a′** were obtained with poor enantioselectivity under the catalysis of $Pd(TFA)_2$/**L11**. Notably, even trisubstituted allenes proved to be reliable partners, preferentially affording products **5b** and **5c** having a quaternary stereocenter with high regioselectivity, though the enantioselectivity was currently unsatisfactory (Scheme 2d).

Migratory insertion of π-allylpalladium complexes into simple alkenes represents a more challenging task. Although strained norbornenes can engage in such a process,[18] attempts

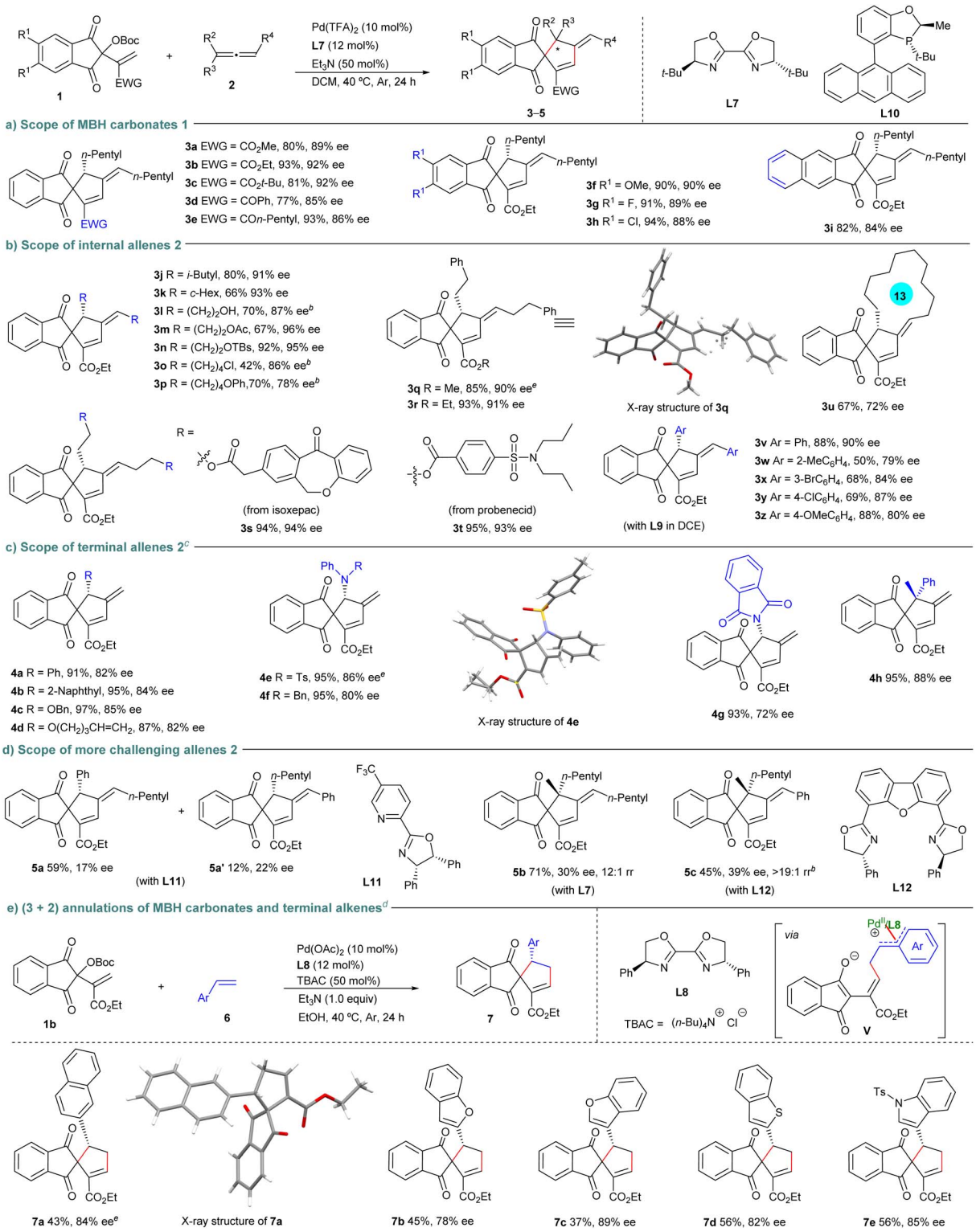


Scheme 2 Asymmetric (3 + 2) annulations of MBH carbonates and diverse allenes[a]. [a]On a 0.1 mmol scale. [b]For 48 h. [c]With **L10** (12 mol%) at rt. [d]With alkene **6** (0.5 mmol), $Pd(OAc)_2$ (10 mol%), **L8** (12 mol%), TBAC (50 mol%) and $Et_3N$ (1.0 equiv) in EtOH (1.0 mL). [e]The absolute configuration of enantiopure **3q**, **4e** and **7a** were determined by X-ray analysis. Other products were assigned by analogy.

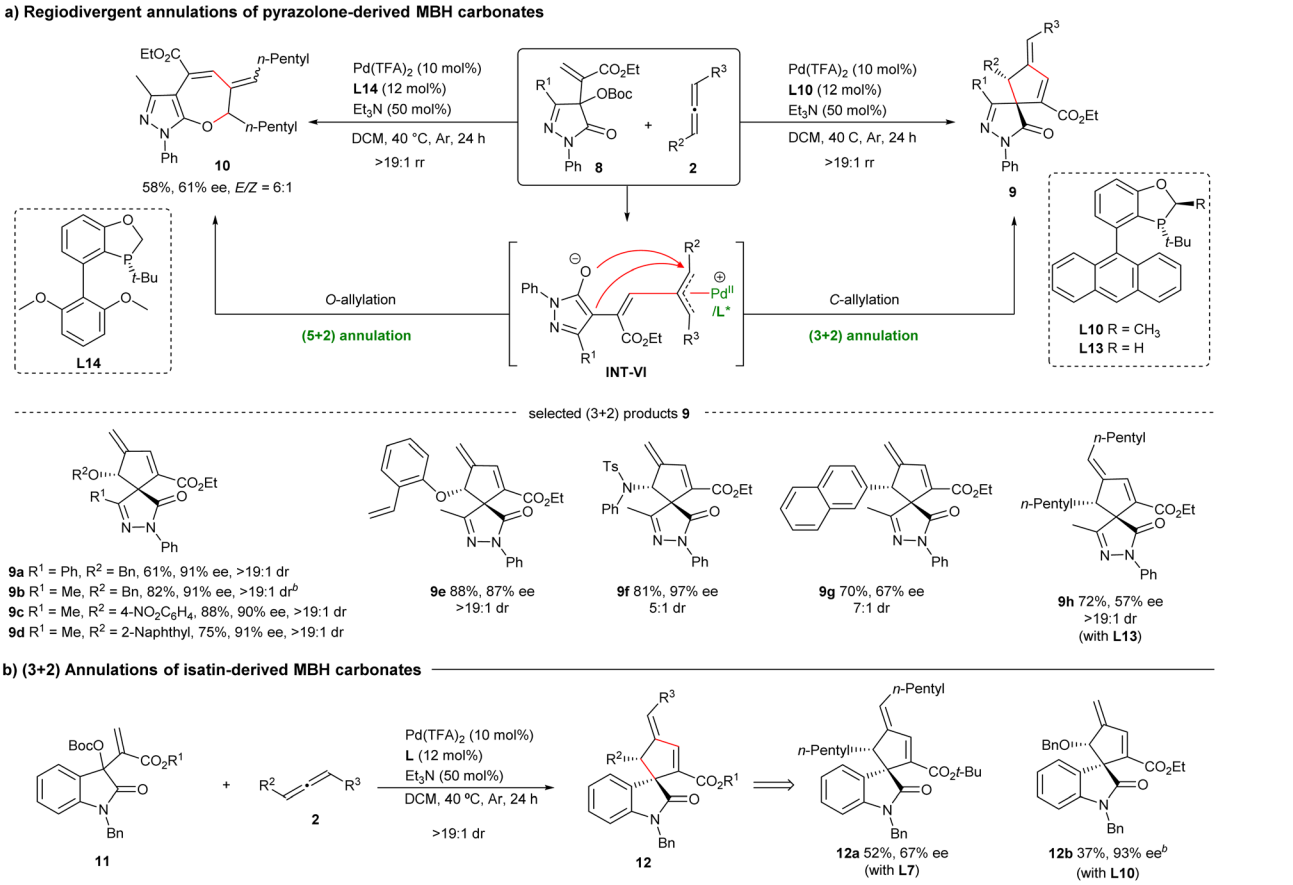


Scheme 3 Exploration of more types of MBH carbonates[a]. [a]On a 0.1 mmol scale. [b]The absolute configurations of enantiopure **9b** was determined by X-ray analysis after conversion to **18**. The relative configuration of **12b** was determined by X-ray analysis after derivatisation, and its absolute configuration was assigned by ECD analysis (see the SI). Other products were assigned by analogy.

to perform migratory insertion of zwitterionic π-allylpalladium species with alkenes all proved unsuccessful due to the high energy barriers involved.[10] Notably, the assembly of MBH carbonate **1b** and 2-vinylnaphthalene **6a** was successful under the catalysis of $Pd(OAc)_2$/**L8**, with tetrabutylammonium chloride (TBAC) as an additive,[19] furnishing (3 + 2) product **7a** with good enantioselectivity, albeit in a fair yield, probably by forming dearomative intermediate **V**.[20] Importantly, other benzo-fused heteroarenes were compatible (products **7b–e**), as summarised in Scheme 2e. Collectively, these reactions well demonstrated the broad applicability of the current approach with respect to diversely substituted allenes as well as terminal alkenes.

To further exhibit the generality of this protocol and construct skeletally diverse products, the MBH carbonates derived from other activated ketones were investigated. As depicted in Scheme 3a, pyrazolone-based MBH carbonates **8** underwent similar (3 + 2) annulations with both terminal and internal allenes efficiently in the presence of $Pd(TFA)_2$/**L10** or **L13**, respectively, affording products **9a–h** bearing two adjacent stereocenters with moderate to good enantioselectivity. Notably, a different regioselective *O*-allylation of intermediate **VI** occurred to deliver (5 + 2) product **10** by using $Pd(TFA)_2$/**L14**, albeit in moderate yield and stereoselectivity. In addition, isatin-based MBH carbonates **11** were also suitable for (3 + 2) annulations with allenes, and products **12a** and **12b** were afforded with moderate data under the catalysis of $Pd(TFA)_2$ with **L7** or **L10**, respectively (Scheme 3b). Regrettably, some aldehyde-derived MBH carbonates and tetrasubstituted allenes were not suitable for current transformation.[16]

## Synthetic transformations

The obtained multifunctional (3 + 2) annulation adducts demonstrate versatile synthetic utility, serving as a valuable platform for accessing structurally diverse architectures. As illustrated in Scheme 4, treating product **9b** with $K_2OsO_4 \cdot 2H_2O$/NMO provided diol **13** with high diastereoselectivity. Interestingly, chemoselective oxidative cleavage of terminal olefin of **9b** with $K_2OsO_4 \cdot 2H_2O/NaIO_4$ furnished ketone **14**, which could be further converted to chiral lactone **15** *via* Baeyer–Villiger rearrangement. Besides, the *exo*-cyclic double bond of **9b** also underwent selective hydrogenation to yield **16**, or sulfur-

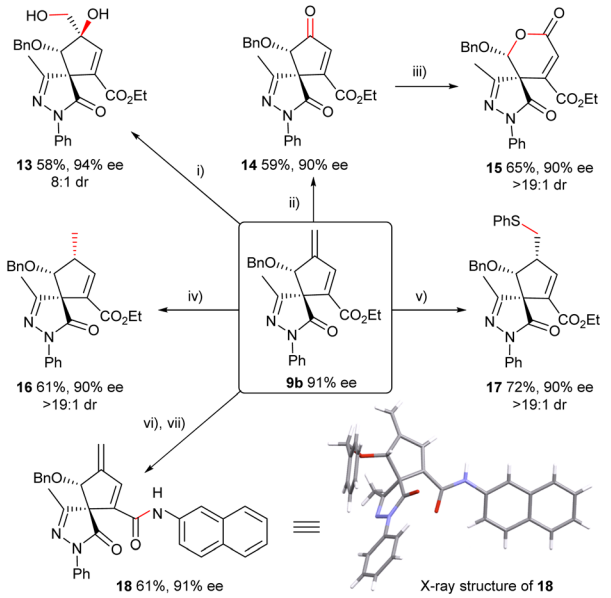


Conditions: i) $K_2OsO_4{\cdot}2H_2O$ (10 mol%), NMO (5.0 equiv), THF/$H_2O$, rt, 12 h. ii) $K_2OsO_4{\cdot}2H_2O$ (10 mol%), $NaIO_4$ (5.0 equiv), THF/$H_2O$, rt, 2 h. iii) *m*-CPBA (2.0 equiv), $NaHCO_3$ (2.0 equiv), DCM, rt, 48 h. iv) Pd/C (10 wt%), $H_2$ balloon, EtOAc, rt, 12 h. v) PhSSPh (0.6 equiv), Rongalite (2.0 equiv), $K_2CO_3$ (1.0 equiv), DMF, rt, 12 h. vi) LiOH (5.0 equiv), THF/MeOH/$H_2O$, 60 °C, 1 h. vii) 2-aminonaphthalene (2.0 equiv), *i*-BuOCOCl (2.0 equiv), *N*-methylmorpholine (2.0 equiv), DCM, rt, 12 h.

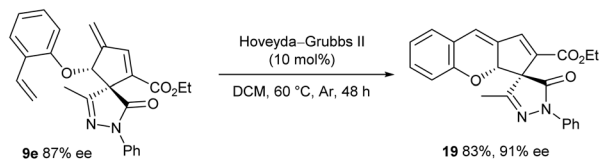


Scheme 4 Synthetic transformations of products.

Michael addition to give **17**,[21] both with exclusive diastereoselectivity. Additionally, the ethyl ester group of **9b** was amenable to hydrolysis followed by condensation with 2-aminonaphthalene to generate amide **18** with retained enantioselectivity. Moreover, a ring-closing metathesis reaction of compound **9e** delivered polycyclic product **19**.

## Mechanism studies

As proposed in Scheme 5a, path A, the key π-allylpalladium complex **INT3** may be generated from the oxidative addition of $Pd^0$ to MBH carbonate **1b**, followed by migratory insertion into simplified allene **2a′**.[11] Alternatively, allene **2a′** might also be activated by $Pd^0$ *via* $\eta^2$-coordination and backdonation based on a Dewar–Chatt–Duncanson model,[12,22] which is indeed supported by DFT calculations. It is found that the HOMO energy of $Pd^0$-$\eta^2$-complex **INT6** (−4.79 eV) is significantly enhanced compared to that of allene **2a′** (−6.87 eV). The nucleophilicity enhanced **INT6** may attack MBH carbonate **1b** to form π-allylpalladium complex **INT3** in a $S_N2'$ fashion (path B).

To figure out which reaction pathway is more favourable, comprehensive DFT calculations were conducted. As shown in Scheme 5b (black line), the energy barrier of oxidative addition of $Pd^0$ to MBH carbonate **1b** *via* **TS1** is 15.5 kcal mol$^{-1}$. Notably, the pendent carbonyl group of 1,3-indandione serves as an additional binding group to facilitate the isomerisation of $\eta^3$-allylpalladium complex **INT1** to slightly more stable $\eta^1$-one **INT2**. Subsequent migratory insertion of **INT2** into allene **2a′** *via* **TS2**, with a free energy barrier of 22.0 kcal mol$^{-1}$, constitutes the rate-determining step and is feasible under current reaction conditions. Although the ester moiety can also serve as a binding group to form **INT2′**, the energy barrier for subsequent migratory insertion into allene **2a′** *via* **TS2′** is apparently higher than that of **TS2** (25.8 *vs.* 22.0 kcal mol$^{-1}$, red line), because of apparent steric hindrance between the ester group and the 1,3-indandione skeleton in **TS2′**, as noted in Scheme 5c. In contrast, the attack of HOMO-raised $Pd^0$-$\eta^2$-complex **INT6** on MBH carbonate **1b** *via* **TS4** features a significantly higher energy barrier of 31.0 kcal mol$^{-1}$ (blue line), indicating it is dynamically infeasible at current reaction temperature. Consequently, the proposed oxidative addition/migratory insertion process is more favourable for the initial assembly of two partners. Moreover, as conjugated polyunsaturated systems are typically required for π-Lewis base catalysis,[22b–d] the successful engagement of styrene-type alkenes **6** in current (3 + 2) annulations (Scheme 2e) provides additional and solid evidence in supporting an oxidative addition/migratory insertion mechanism.

The strong electron-withdrawing effect of both 1,3-indandione and the π-allylpalladium complex renders the β′-H of **INT3** highly acidic, which can be easily deprotonated by the *in situ* generated *t*-butoxide anion to deliver the more stable intermediate **INT4** with a significant exotherm of 35.0 kcal mol$^{-1}$. In addition, an outer-sphere allylic alkylation *via* **TS3**, with an energy barrier of only 5.2 kcal mol$^{-1}$, can smoothly occur to provide product **3b′** after ligand exchange.[16]

As outlined in Scheme 6a, racemic **2h** was recovered when 2.0 equivalents of **2h** were used, indicating that kinetic resolution of racemic allene **2h** is not involved in this transformation. Instead, the dynamic kinetic transformation (DKT) of the π-allylpalladium species **IV** appears to be operative.[12] Consequently, further calculations were conducted to elucidate the origin of enantioselectivity. Both **INT4** and ***ent*-INT4** would be generated *via* migratory insertion of **INT2** into racemic **2a′** followed by deprotonation. As depicted in Scheme 6b, a comparative geometry analysis reveals that the distance between $H^1$ and $H^2$ in **TS3** (2.15 Å) is longer than that between $H^3$ and $H^4$ in ***ent*-TS3** (2.07 Å), indicating a greater 1,3-strain between the adjacent H atom and $CH_3$ moiety in ***ent*-TS3**. This steric repulsion leads to the free energy of ***ent*-TS3** being 2.2 kcal mol$^{-1}$ higher than that of **TS3**, suggesting that ***ent*-INT4** would undergo dynamic kinetic transformation (DKT) into **INT4** *via* π–σ–π isomerisation, thus producing (*R*)-**3b′** predominantly.[23] This theoretical prediction is in agreement with the experimental observations. The above DFT calculations identify migratory insertion as the rate-determining step, and intramolecular allylation as the enantioselectivity-determining step.

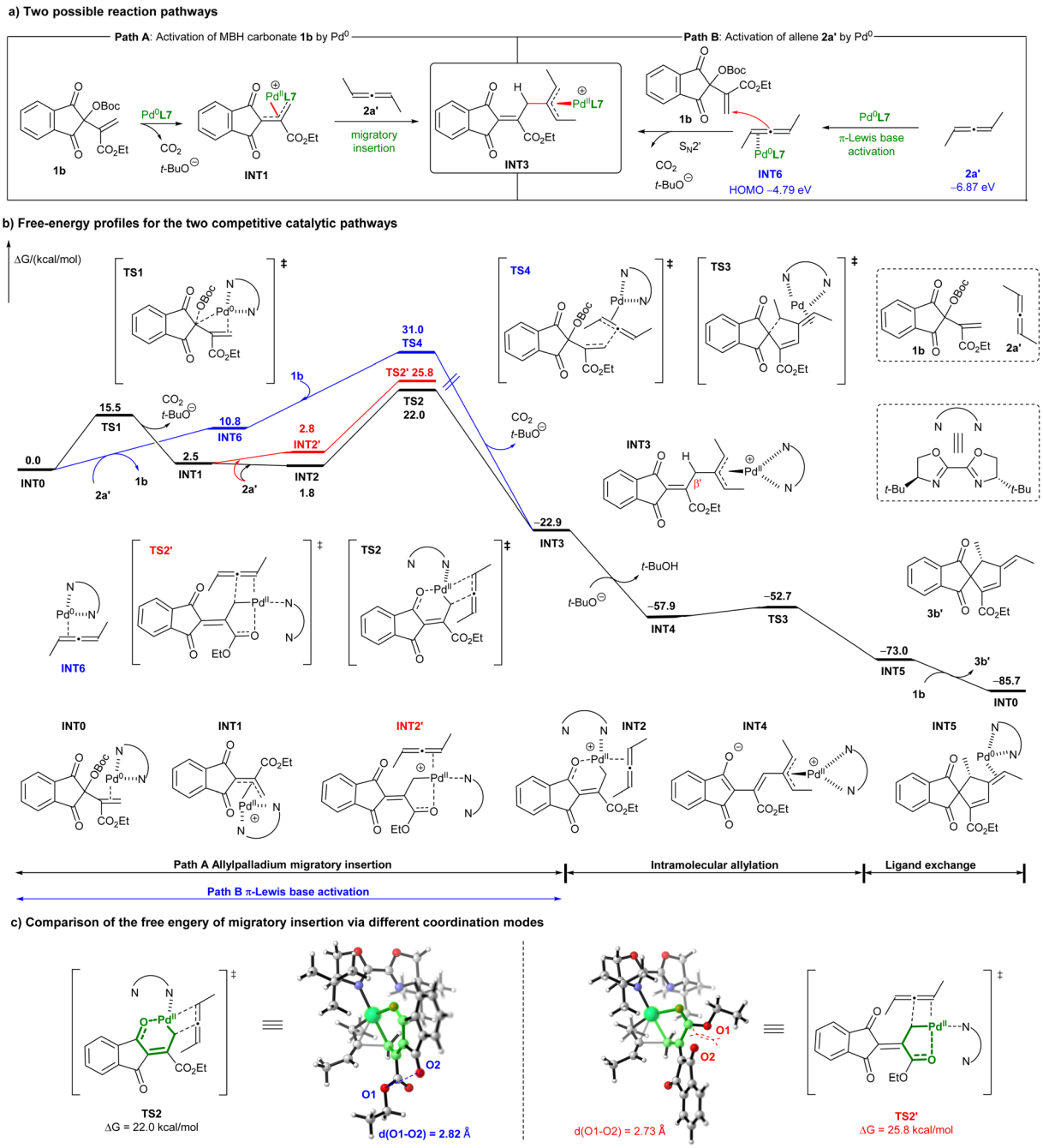


Scheme 5 Mechanism studies on different activation pathways.

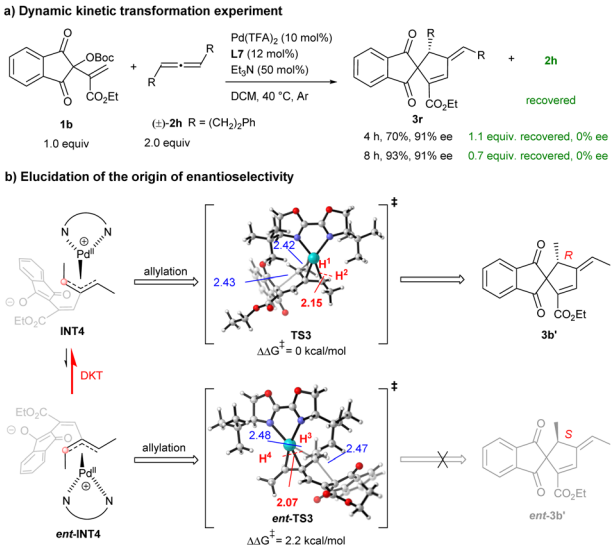


Scheme 6 Elucidation of the enantioselectivity.

## Conclusions

In summary, with the assistance of experimental results and density functional theory calculations, we demonstrated that the functionalised π-allylpalladium complexes, generated by oxidative addition of $Pd^0$ to the Morita–Baylis–Hillman carbonates from activated ketones, could readily isomerise to their $\eta^1$-form *via* ligation with the pendent carbonyl group, which enabled migratory insertion into diverse allenes and styrene-type alkenes. Subsequent vinylogous deprotonation and intramolecular allylic alkylation furnished (3 + 2) annulation products. This protocol featured substantial substrate scope and good functional group compatibility, delivering a diversity of spirocyclic frameworks with moderate to excellent regio-, chemo-, and stereoselectivity. As a result, a novel transformative paradigm for multifunctional MBH carbonates has been established *via* migratory insertion of the *in situ* formed non-zwitterionic π-allylpalladium species, rendering their unprecedented annulations with electron-neutral unsaturated systems—previously inaccessible under Lewis base catalysis. Further expansion studies of these Morita–Baylis–Hillman carbonates with other types of unsaturated systems are under investigation, and the results will be reported in due course.

## Author contributions

The manuscript was written through contributions of all authors. All authors have given approval to the final version of the manuscript.

## Conflicts of interest

There are no conflicts to declare.

## Data availability

CCDC 2473163–2473167 (**3q**, **4e**, **7a**, **18** and the derivative of racemic **12b**) contain the supplementary crystallographic data for this paper.[24a–e]

The data that support the findings of this study are available in the supplementary information (SI) or on request from the corresponding author. Supplementary information: experimental procedures, spectroscopic data for new compounds, NMR, HRMS spectra and HPLC chromatograms, and CIF files of enantiopure products **3q**, **4e**, **7a**, **18** and the derivative of racemic **12b**. See DOI: https://doi.org/10.1039/d5sc06910f.

## Acknowledgements

This project was supported by the Sichuan Science and Technology Program (2025ZNSFSC0124). We thank Dr Meng Yang from College of Chemistry, Sichuan University, for X-ray diffraction analysis, and Dr Wan-Shu Wang from West China School of Pharmacy, Sichuan University, for NMR analysis.

## Notes and references

1 For selected reviews, see: (*a*) B. M. Trost, *Chem. Pharm. Bull.*, 2002, **50**, 1–14; (*b*) S. Parisotto and A. Deagostino, *Synthesis*, 2019, **51**, 1892–1912; (*c*) O. Pàmies, J. Margalef, S. Cañellas, J. James, E. Judge, P. J. Guiry, C. Moberg, J.-E. Bäckvall, A. Pfaltz, M. A. Pericàs and M. Diéguez, *Chem. Rev.*, 2021, **121**, 4373–4505; (*d*) L. Mohammadkhani and M. M. Heravi, *Chem. Rec.*, 2021, **21**, 29–68; (*e*) B. Niu, Y. Wei and M. Shi, *Org. Chem. Front.*, 2021, **8**, 3475–3501; (*f*) B. Xu, Q. Wang, C. Fang, Z.-M. Zhang and J. Zhang, *Chem. Soc. Rev.*, 2024, **53**, 883–971.

2 For selected reviews, see: (*a*) N. A. Butt and W. Zhang, *Chem. Soc. Rev.*, 2015, **44**, 7929–7967; (*b*) J. Qian and G. Jiang, *Curr. Catal.*, 2017, **6**, 25–30; (*c*) Q.-Z. Li, Y. Liu, M.-Z. Li, X. Zhang, T. Qi and J.-L. Li, *Org. Biomol. Chem.*, 2020, **18**, 3638–3648; (*d*) Y. You, Q. Li, Y.-P. Zhang, J.-Q. Zhao, Z.-H. Wang and W.-C. Yuan, *ChemCatChem*, 2022, **14**, e202101887.

3 For selected reviews, see: (*a*) S. E. Mann, L. Benhamou and T. D. Sheppard, *Synthesis*, 2015, **47**, 3079–3117; (*b*) P. Wang and L. Gong, *Acc. Chem. Res.*, 2020, **53**, 2841–2854.

4 For selected reviews, see: (*a*) G. Li, X. Huo, X. Jiang and W. Zhang, *Chem. Soc. Rev.*, 2020, **49**, 2060–2118; (*b*) G. Cera and G. Maestri, *ChemCatChem*, 2022, **14**, e202200295; (*c*) L. Li, S. Wang, A. Jakhar and Z. Shao, *Green Synth. Catal.*, 2023, **4**, 124–134.

5 For a selected review, see: (*a*) R. A. Fernandes and J. L. Nallasivam, *Org. Biomol. Chem.*, 2019, **17**, 8647–8672; for recent selected examples, see: ; (*b*) Z. Yang and J. J. Wang, *Angew. Chem., Int. Ed.*, 2021, **60**, 27288–27292; (*c*) Y. Jin, Y. Jing, C. Li, M. Li, W. Wu, Z. Ke and H. Jiang, *Nat. Chem.*, 2022, **14**, 1118–1125; (*d*) J. Liu, W.-B. Cao and S.-L. You, *Chem*, 2024, **10**, 1295–1305; (*e*) S. H. M. Kaster, L. Zhu, W. L. Lyon, R. Ma, S. E. Ammann and M. C. White, *Science*, 2024, **385**, 1067–1076.

6 For selected reviews and examples, see: (*a*) K. Spielmann, G. Niel, R. M. de Figueiredo and J. Campagne, *Chem. Soc. Rev.*, 2018, **47**, 1159–1173; (*b*) S.-F. Zhu, X.-C. Qiao, Y.-Z. Zhang, L.-X. Wang and Q.-L. Zhou, *Chem. Sci.*, 2011, **2**, 1135–1140; (*c*) T. Mita, Y. Higuchi and Y. Sato, *Chem.–Eur. J.*, 2015, **21**, 16391–16394; (*d*) Y. Li, P. Chen,

Z.-C. Chen, W. Du, Q. Ouyang and Y.-C. Chen, *Org. Chem. Front.*, 2021, **8**, 5418–5423.

7 For selected reviews, see: (*a*) Y. Ping, Y. Li, J. Zhu and W. Kong, *Angew. Chem., Int. Ed.*, 2019, **58**, 1562–1573; (*b*) R.-X. Liang and Y.-X. Jia, *Acc. Chem. Res.*, 2022, **55**, 734–745; (*c*) G. Zhao, W. Li and J. Zhang, *Chem.–Eur. J.*, 2024, **30**, e202400076.

8 R. Hughes and J. Powell, *J. Am. Chem. Soc.*, 1972, **94**, 7723–7732.

9 (*a*) B. M. Trost, Z. Huang and G. M. Murhade, *Science*, 2018, **362**, 564–568; (*b*) B. M. Trost and Z. Huang, *Angew. Chem., Int. Ed.*, 2019, **58**, 6396–6399; (*c*) W. Chai, Q. Zhou, W. Ai, Y. Zheng, T. Qin, X. Xu and W. Zi, *J. Am. Chem. Soc.*, 2021, **143**, 3595–3603; (*d*) W. Zhang, P.-C. Zhang, Y.-L. Li, H.-H. Wu and J. Zhang, *J. Am. Chem. Soc.*, 2022, **144**, 19627–19634.

10 Y. Zou, S. Chen and K. N. Houk, *J. Am. Chem. Soc.*, 2019, **141**, 12382–12387.

11 (*a*) D. C. Witkowski, M. S. McVeigh, G. M. Scherer, S. M. Anthony and N. K. Garg, *J. Am. Chem. Soc.*, 2023, **145**, 10491–10496; (*b*) H. Xu and S. Ma, *Angew. Chem., Int. Ed.*, 2023, **62**, e202213676.

12 R.-J. Yan, Y. Hu, L. Zhu, J. Zhang, Q. Wang, J.-Y. Huang, Z.-C. Chen, Q. Ouyang, W. Du and Y.-C. Chen, *ACS Catal.*, 2024, **14**, 12824–12832.

13 For selected reviews, see: (*a*) P. Xie and Y. Huang, *Org. Biomol. Chem.*, 2015, **13**, 8578–8595; (*b*) Z.-C. Chen, Z. Chen, W. Du and Y.-C. Chen, *Chem. Rec.*, 2020, **20**, 541–555; (*c*) A. Calcatelli, A. CherubiniCelli, E. Carletti and X. Companyo, *Synthesis*, 2020, **52**, 2922–2939; (*d*) X.-H. Duan, H.-R. Du and Y.-X. Song, *Org. Chem. Front.*, 2025, **12**, 2076–2130.

14 Z.-L. He, P. Chen, Z.-C. Chen, W. Du and Y.-C. Chen, *Org. Lett.*, 2022, **24**, 100–104.

15 For selected reviews, see: (*a*) R. C. Fuson, *Chem. Rev.*, 1935, **16**, 1–27; (*b*) C. Curti, L. Battistini, A. Sartori and F. Zanardi, *Chem. Rev.*, 2020, **120**, 2448–2612.

16 For more details, see the SI.

17 (*a*) A. M. Trzeciak, Z. Ciunik and J. J. Ziółkowski, *Organometallics*, 2002, **21**, 132–137; (*b*) J. Bajohr, A. G. Diallo, A. Whyte, S. Gaillard, J. Renaud and M. Lautens, *Org. Lett.*, 2021, **23**, 2797–2801.

18 (*a*) B. M. Trost and S. Schneider, *J. Am. Chem. Soc.*, 1989, **111**, 4430–4433; (*b*) B. M. Trost and H. Urabe, *Tetrahedron Lett.*, 1990, **31**, 615–618; (*c*) K. Ohe, H. Matsuda, T. Ishihara, S. Ogoshi, N. Chatani and S. Murai, *J. Org. Chem.*, 1993, **58**, 1173–1177; (*d*) I. Ikeda, A. Ohsuka, K. Tani, T. Hirao and H. Kurosawa, *J. Org. Chem.*, 1996, **61**, 4971–4974.

19 (*a*) K. Fagnou and M. Lautens, *Angew. Chem., Int. Ed.*, 2002, **41**, 26–47; (*b*) T. Cantat, N. Agenet, A. Jutand, R. Pleixats and M. Moreno-Manas, *Eur. J. Org Chem.*, 2005, 4277–4286; (*c*) J. G. Knight, P. A. Stoker, K. Tchabanenko, S. J. Harwood and K. W. M. Lawrie, *Tetrahedron*, 2008, **64**, 3744–3750; (*d*) M. A. Lowe, M. Ostovar, S. Ferrini, C. C. Chen, P. G. Lawrence, F. Fontana, A. A. Calabrese and V. K. Aggarwal, *Angew. Chem., Int. Ed.*, 2011, **50**, 6370–6374; (*e*) C. B. E. Chao, Q. H. Pham, C. Richardson, S. G. Pyne and C. J. T. Hyland, *J. Org. Chem.*, 2024, **89**, 13744–13755.

20 For selected examples, see: (*a*) S. Tabuchi, K. Hirano and M. Miura, *Angew. Chem., Int. Ed.*, 2016, **55**, 6973–6977; (*b*) K. J. Schwarz, C. Yang, J. W. B. Fyfe and T. N. Snaddon, *Angew. Chem., Int. Ed.*, 2018, **57**, 12102–12105; (*c*) S. Sun, Q. Zhang and W. Zi, *ACS Catal.*, 2023, **13**, 12952–12959.

21 W. Guo, G. Lv, J. Chen, W. Gao, J. Ding and H. Wu, *Tetrahedron*, 2010, **66**, 2297–2300.

22 (*a*) G. J. Kubas, *J. Organomet. Chem.*, 2001, **635**, 37–68; (*b*) B.-X. Xiao, B. Jiang, R.-J. Yan, J.-X. Zhu, K. Xie, X.-Y. Gao, Q. Ouyang, W. Du and Y.-C. Chen, *J. Am. Chem. Soc.*, 2021, **143**, 4809–4816; (*c*) Q. He, L. Zhu, Z.-H. Yang, B. Zhu, Q. Ouyang, W. Du and Y.-C. Chen, *J. Am. Chem. Soc.*, 2021, **143**, 17989–17994; for a perspective, see: ; (*d*) Z.-C. Chen, Q. Ouyang, W. Du and Y.-C. Chen, *J. Am. Chem. Soc.*, 2024, **146**, 6422–6437.

23 For selected reviews and examples, see: (*a*) J. Steinreiber, K. Faber and H. Griengl, *Chem.–Eur. J.*, 2008, **14**, 8060–8072; (*b*) V. Bhat, E. R. Welin, X. Guo and B. M. Stoltz, *Chem. Rev.*, 2017, **117**, 4528–4561; (*c*) B. M. Trost, D. B. Horne and M. J. Woltering, *Angew. Chem., Int. Ed.*, 2003, **42**, 5987–5990; (*d*) B. M. Trost, M. R. Machacek and H. C. Tsui, *J. Am. Chem. Soc.*, 2005, **127**, 7014–7024; (*e*) J. Zhang, X. Huo, J. Xiao, L. Zhao, S. Ma and W. Zhang, *J. Am. Chem. Soc.*, 2021, **143**, 12622–12632.

24 (*a*) CCDC 2473163: Experimental Crystal Structure Determination, 2025, DOI: **10.5517/ccdc.csd.cc2p0jgq**; (*b*) CCDC 2476164: Experimental Crystal Structure Determination, 2025, DOI: **10.5517/ccdc.csd.cc2p3n8r**; (*c*) CCDC 2476165: Experimental Crystal Structure Determination, 2025, DOI: **10.5517/ccdc.csd.cc2p3n9s**; (*d*) CCDC 2476166: Experimental Crystal Structure Determination, 2025, DOI: **10.5517/ccdc.csd.cc2p3nbt**; (*e*) CCDC 2476167: Experimental Crystal Structure Determination, 2025, DOI: **10.5517/ccdc.csd.cc2p3ncv**.